

# Measurement of the Force and Torque Produced in the Calcium Response of Reactivated Rat Sperm Flagella

Mark J. Moritz, Kathleen A. Schmitz, and Charles B. Lindemann\*

*Department of Biological Sciences, Oakland University, Rochester, Michigan*

Rat sperm that are demembrated with Triton X-100 and reactivated with Mg-ATP show a strong mechanical response to the presence of free calcium ion. At  $pCa < 4$ , the midpiece region of the flagellum develops a strong and sustained curvature that gives the cell the overall appearance of a fishhook [Lindemann and Goltz, 1988: *Cell Motil. Cytoskeleton* 10:420–431]. In the present study, the force and torque that maintain the calcium-induced hook have been examined quantitatively. In addition, full-length and shortened flagella were manipulated to evaluate the plasticity of the hooks and determined the critical length necessary for maintaining the curvature. The hooks were found to be highly resilient, returning to their original configuration (>95%) after being straightened and released. The results from manipulating the shortened flagella suggest that the force holding the hook in the curved configuration is generated in the basal 60  $\mu\text{m}$  of the flagellum. The force required to straighten the calcium-induced hooks was measured with force-calibrated glass microprobes, and the bending torque was calculated from the measured force. The force and torque required to straighten the flagellum were found to be proportional to the change in curvature of the hooked region of the flagellum, suggesting an elastic-like behavior. The average torque to open the hooks to a straight position was  $2.6 (\pm 1.4) \times 10^{-7}$  dyne  $\times$  cm ( $2.6 \times 10^{-14}$  N  $\times$  m) and the apparent stiffness was  $4.3 (\pm 1.3) \times 10^{-10}$  dyne  $\times$  cm<sup>2</sup> ( $4.3 \times 10^{-19}$  N  $\times$  m<sup>2</sup>). The stiffness of the hook was determined to be approximately one quarter the rigor stiffness of a rat sperm flagellum measured under comparable conditions. *Cell Motil. Cytoskeleton* 49:33–40, 2001. © 2001 Wiley-Liss, Inc.

**Key words:** axoneme; cilia; dynein; outer dense fibers; hyperactivation; detergent-extracted models; glass microprobes

## INTRODUCTION

Triton X-100 extracted rat sperm exhibit a strong mechanical response to elevated free  $\text{Ca}^{+2}$  ion in the presence of ATP [Lindemann et. al., 1987; Lindemann and Goltz, 1988]. The response consists of the formation of a fishhook-like curve in the midpiece region of the sperm flagellum, which is quite stable and persist whether or not the flagellum is actively beating. When the flagellum is fully reactivated to motility with a calcium hook present, the beating pattern strongly resembles the motility called “hyperactivation” in live rat sperm [Lindemann and Goltz, 1988]. This connection is also supported by reports that a calcium influx accompanies the transition to hyperactivated motility in the live sperm [Fraser, 1987; Suarez et al., 1993].

The calcium response is a well-documented behavior that is observed in a wide spectrum of eukaryotic flagella and cilia in addition to mammalian sperm [Walter and Satir, 1978; Wais-Steider and Satir, 1979; Brokaw, 1979, 1987]. In fact, the response was first observed in the cilia and flagella of invertebrate organisms [Naitoh, 1968, 1969; Nai-

Contract grant sponsor: National Science Foundation; Contract grant number: MCB-9722822.

\*Correspondence to: Dr. Charles B. Lindemann, Dept. of Biological Sciences, Oakland University, Rochester, MI 48309-4476.  
E-mail: lindeman@oakland.edu

Received 19 September 2000; Accepted 26 January 2001

toh and Kaneko, 1972; Brokaw et al., 1974; Satir, 1975; Tsuchiya, 1976, 1977; Brokaw and Goldstein, 1979; Gibbons, 1980; Gibbons and Gibbons, 1980]. In these organisms it has been shown to play a role in chemotactic and phototactic responses [Miller and Brokaw, 1970; Schmidt and Eckert, 1976; Hegemann and Bruck, 1989]. In spite of its widespread distribution, its importance in mammalian fertilization, and the chemotactic and phototactic responses of ciliate and flagellate organisms, little is known about the underlying mechanism that produces the calcium response. It is likely that the response mechanism is a function of the 9+2 axoneme that is common to most cilia and flagella, since the response can be observed in the simple flagella of sea urchin sperm and the simple cilia of invertebrates. If this is the case, we would expect that dynein, the motor protein of the axoneme, is responsible for the motive force that produces the hook. However, there is presently little physical data available on the strength and the mechanical properties of the hook response that might be used to evaluate the underlying mechanism.

In order to gain a better physical description of the nature of a calcium hook, we have used calibrated glass microprobes to measure the force required to unbend the flagellum of a rat sperm during a calcium-induced response. This has permitted us to directly measure the force that the flagellum is able to generate by the hook-forming mechanism. We have also been able to estimate the length of flagellum needed to maintain the hook by serially shortening the flagellum and measuring the resultant curvature. Estimates of the bending torque acting on the flagellum and the apparent stiffness of the flagellum are also presented. The relationship of the bending torque to the curvature of the flagellum has been examined to see if it is compatible with an elastic model or a dynamic model for the production of the bending torque in the formation and maintenance of the hook.

## MATERIALS AND METHODS

### Microprobe Production and Calibration

Microprobes were made and force-calibrated following the methods detailed in Schmitz et al. [2000]. Briefly, force-measuring probes were made by pulling 1-mm borosilicate glass rod (Sutter Instrument Co.) to a taper length of 9 mm, while probes for cutting were pulled to a taper length of 6 mm. Both probe types had a final tip diameter of  $< 1 \mu\text{m}$ .

Horizontally mounted probes were calibrated by electrostatically adhering  $\sim 45\text{-}\mu\text{m}$  polystyrene beads (Polysciences, Inc., Warrington, PA) to the tip of the probe and measuring the resultant probe displacement with an ocular micrometer [Van Buren et al., 1994]. The density of the beads is known ( $1.05 \text{ g/cm}^3$ ), while the

**TABLE I. Calibration Data for Glass Microprobes**

Probe	No. of calibration points	Pre/post usage <sup>a</sup>	No. of force measurements	Mean force of calibrations (dynes/ $\mu\text{m}$ )
A	12	Post	1	$2.60 \times 10^{-6}$
B	15	Post	7	$1.68 \times 10^{-6}$
C	10	Pre	2	$8.76 \times 10^{-6}$
D	9	Pre	2	$2.94 \times 10^{-6}$
E	12	Post	1	$6.08 \times 10^{-6}$
F	19	Post	6 <sup>b</sup>	$2.98 \times 10^{-6}$
G	13	Post	2 <sup>b</sup>	$1.72 \times 10^{-6}$

<sup>a</sup>Pre/post-usage defines when calibrations were performed in relation to experiments.

<sup>b</sup>Rigor stiffness measurements only.

actual size of each bead and its location on the probe was determined microscopically. With this information, it was possible to accurately determine the force applied to the probe by the attached bead(s). The mean probe stiffness value from a number of individual calibration points for each probe used in the study is presented in Table I. Probe stiffness values in Table I are extrapolated to the probe tip by regression analysis from the individual calibrations using the method in Schmitz et al. [2000].

### Sperm Preparation

Sexually mature male Sprague-Dawley rats (Charles River Laboratories, Wilmington, MA) were euthanized by  $\text{CO}_2$  asphyxiation. Sperm were removed from the caudal epididymis by opening it with a razor and gently expressing the sperm onto the surface of a plastic petri dish. The cells were immediately covered with sodium citrate buffer (0.097 M sodium citrate, 2 mM fructose and 5 mM magnesium sulfate, pH 7.4). The sperm were allowed to disperse into the fluid and the final suspension was diluted to a total of 4 ml with additional citrate buffer. This was used as the stock sperm solution.

### Reactivation

For each reactivation, 10–30  $\mu\text{l}$  of stock sperm solution was added to 3 ml of a reactivation mixture in a cell culture dish. The final concentration of sperm in the stock solution varied for individual experiments. Thus, the amount added to a reactivation was adjusted such that optimal manipulation and visualization of an individual cell was achieved. The reactivation mixture (pH 7.8) contained 0.024 M potassium glutamate, 0.132 M sucrose, 0.02 M Tris-HCl (Fisher Scientific, Itasca, IL), 1 mM dithiothreitol (DTT) (Roche, Indianapolis, IN), 2 mM  $\text{MgSO}_4$ , 0.5 mM EGTA, and 0.1% Triton X-100 (Pierce, Rockford, IL). After initial observation for the absence of motility, ATP (Fisher Scientific) and cAMP (Roche) were added to final concentrations of 0.3 mM and 3  $\mu\text{M}$ , respectively. Lastly, 1 mM  $\text{CaCl}_2$  (final concentration) was added to induce the

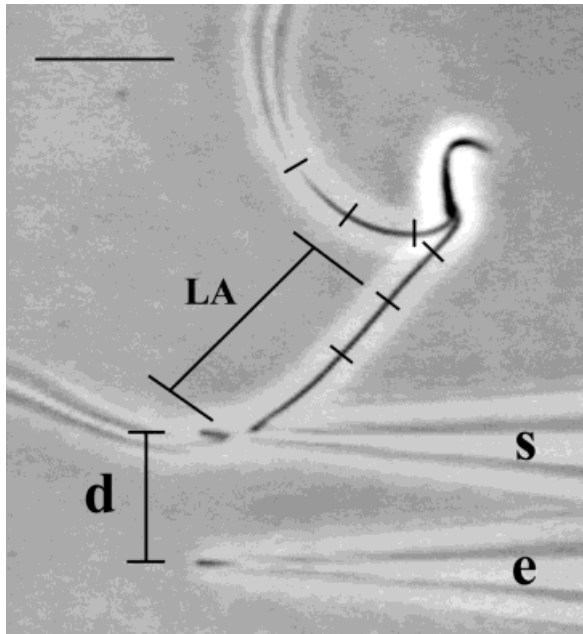


Fig. 1. Measurement of force produced by a rat sperm flagellum in a  $\text{Ca}^{+2}$ -induced hook. An image of a  $\text{Ca}^{+2}$ -treated rat sperm flagellum, with a microprobe at equilibrium, was overlaid by an image of the same flagellum one frame before the flagellum was released from the probe. e, Position of the microprobe at equilibrium; S, location of the same probe before losing contact with the probe; LA, lever arm length. The markings on the flagella indicate the region where radius of curvature measurements were made. d, displacement of the microprobe. Bar = 20  $\mu\text{m}$ .

“fishhook” response. This corresponds to a free  $\text{Ca}^{+2}$  concentration of  $1.7 \times 10^{-4}$  M. After a sperm responds to  $\text{Ca}^{+2}$ , the hooked midpiece region seldom shows active motility. The distal portion of the flagellum will sometimes continue to beat or jitter, but the hook is usually stationary, allowing the manipulation procedures described below. Reactivated sperm were gently pipetted into a glass slide chamber with an opening of  $1 \times 3$  cm. In order to make the sperm heads adhere to the slide the chamber, it was first washed with 0.05 M KOH, then rinsed with distilled water, washed with 100% acetone, and lastly rinsed with distilled water. This chamber was accessible to micromanipulation when placed on an Olympus IMT-2 microscope.

To measure the stiffness of the flagellum in rigor, the same extraction medium and sperm dilution was used but ATP, cAMP, and  $\text{Ca}^{+2}$  were not added.

### Curvature Measurements

Due to the extreme curvature of the flagellum in the first 6  $\mu\text{m}$  from the head/tail junction, this segment was not used to obtain radius of curvature measurements of the  $\text{Ca}^{+2}$  hooked flagellum. Instead, the region from 6–26  $\mu\text{m}$  on the flagellum was marked on the tracings

and used consistently as the standard for measurement as shown in Figure 1. To measure the radius of curvature, computer-generated concentric circles of known radius (cm) were matched to the curve of the flagellum at the midpoint of the 20- $\mu\text{m}$  flagellar segment marked on the tracings [Holcomb-Wygle et al., 1999], results were corrected for screen magnification and converted to radians/cm. The radius of curvature of the  $\text{Ca}^{+2}$ -induced curve increased distally along the flagellum. To verify the results of matching a single circle to the 20- $\mu\text{m}$  segment, the mean radius of curvature measurement of the 10- $\mu\text{m}$  segments proximal and distal to the midpoint was also obtained and supported the initial measurements.

### Force Measurements

To minimize extraneous probe oscillation due to vibration, all experiments were performed on a Micro-g vibration isolation table (Technical Manufacturing Corp., Peabody, MA). Experiments were viewed with phase contrast illumination and videotaped with a Mitsubishi S-VHS video recorder and a GBC 505-E CCD camera (CCTV Corp.) mounted on the microscope. Data were obtained by making tracings of the videotaped recordings using the jog shuttle feature of the VCR at a framing rate of 30 frames per second.

Sperm were selected for manipulations that were adhered to the glass slide by their heads, showed unobstructed movement of the flagellum, and exhibited the “fishhook” response to  $\text{Ca}^{+2}$ . Movement of the microprobe was controlled by a de Fonbrune type joystick-operated micromanipulator (Technical Products International Inc., St. Louis, MO).

In our original attempts at force measurement, microprobes were used to unbend/open up the hook of multiple individual cells. Hooks were opened by manipulation to a point where the tip of the microprobe rested against the unbent flagellum. At this time, the experimenter’s hands were removed from the manipulator and the cell would often snap free of the microprobe on its own. In instances when the cell would not come free of the probe on its own, the microscope stage was moved either down or laterally, which allowed for release to occur. The position of the probe following release was considered to be the equilibrium position. Displacement of the probe was determined by measuring the distance between the equilibrium position of the probe and the position of the probe just prior to release from the flagellum.

In subsequent experiments, we found it was possible to continuously monitor the relationship between torque and curvature change using a single cell. To accomplish this, the tip of the probe was manipulated to a position on the flagellum that would allow the hook to be unbent (opened up) by the lateral movement of the



Fig. 2. Progressive displacement of a force-calibrated microprobe by a  $\text{Ca}^{+2}$ -induced rat sperm flagellum. A Triton X-100 extracted rat sperm was reactivated with 1 mM ATP and then treated with 1 mM  $\text{Ca}^{+2}$  to induce the formation of a "hook." The sperm and slide are moved upward on an intersecting path with a stationary force-cal-

ibrated microprobe. As the sperm moves upward, the flagellum catches on the probe and displaces the microprobe while simultaneously opening up the calcium hook. Upon release the microprobe returns to its original position and the sperm recoils back into the hooked configuration. Bar = 50  $\mu\text{m}$ .

sperm relative to the probe. After this initial positioning of the probe, the experimenter's hands were removed from the manipulator and the stage was moved slowly in a lateral direction, thereby opening the hooked region of the flagellum with the probe. The microprobe generally slid slowly and smoothly along the flagellum as the hook was progressively opened, as seen in Figure 2. Those cells in which the probe moved rapidly down the flagellum were excluded from the data. This method of opening a rat  $\text{Ca}^{+2}$  hook allowed measurements of a single cell's curvature change to be obtained at various positions of the probe as the hook was opened. The corresponding displacement of the probe from its equilibrium point could then be measured at each probe position.

In most instances, a correction factor was necessary to more accurately calculate the relationship between torque and curvature change. The curvature of the hook was measured at a position  $\sim 16 \mu\text{m}$  from the head/tail junction, this being the midpoint of the flagellar segment used to measure radius of curvature. The lever arm between this point and the contact point with the microprobe was often considerably off from parallel with the axis of the microprobe. Therefore, the displacing force exerted by the flagellum on the probe was reduced due to the fact that some of the applied force was off axis to the microprobe. To correct for this, the angle of the lever arm to the axis of the probe was measured using a protractor. The corrected force was found by dividing the measured force value by the cosine of the intersection angle (as illustrated in Fig. 2). Angles ranged from  $0^\circ$  to  $52^\circ$ .

### Length Vs. Curvature and Elasticity Experiments

Sperm cells that exhibited a strong response to  $\text{Ca}^{+2}$  were shortened with a knife-like microprobe to various flagellar lengths. The length of the shortened flagellum was determined by bending a piece of flexible wire into the shape of the traced cell, measuring this length of wire, and correcting for screen magnification. A

radius of curvature measurement was obtained for each shortened flagellum. However, these measurements could not be made on cells that had been clipped to lengths less than  $26 \mu\text{m}$ , as this was the minimum length required for our standard of measurement. The data was then normalized by dividing the measured curvature (radians/cm) of each clipped flagellar segment by the original curvature of that flagellum at full length.

To determine the resiliency of these shortened flagella exhibiting the  $\text{Ca}^{+2}$  response, microprobes were used to unbend the hook and allow the cell to "snap back." Tracings and radius of curvature measurements were obtained for each cut flagellum before unbending the hook, and again following the release of the flagellum.

### Video Microscopy

To compose Figure 1, videotaped sequence of an experiment was digitized using PowerComputing's PowerTower Pro 225 (Round Rock, TX) with MacIntosh Media 100 hardware and software. Figure 2 was digitized using a Dell workstation 220 equipped with Matrox's Meteor II M/C frame grabber and Inspector 3.0 software (Dorval, Quebec, Canada). From the sequence, an image was selected to show the position of the probe one frame before losing contact with the flagellum and another with the probe at the equilibrium position. The background on these images was reduced (threshold mapping changed from 250 to 150). Transparency film prints of the images were overlaid and aligned. The result was scanned with an Agfa Duoscan T1200 scanner and Adobe Photoshop 4.0.

## RESULTS

Triton X-100 extracted rat sperm that showed strong  $\text{Ca}^{+2}$  induced hooks (average 615 radians/cm, range 270–910 radians/cm) were positioned on a micro-

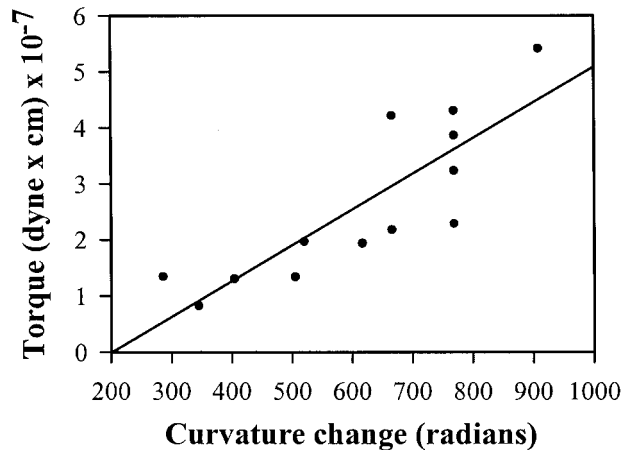


Fig. 3. A scatter plot of the torque required to straighten a calcium-hook vs. the initial curvature of the hook. The plot displays data for 13 different cells and demonstrates that generally more torque is required to open up a tighter hook. It is a relationship with some scatter, which shows that the torque is not uniform from one sperm to another. This is not especially surprising, as there is substantial variation in the shape of the flagella and the tilt angle of the flagellum with the head, all suggesting individual variability.

scope slide such that the sperm heads adhered to the slide with their head positioned roughly perpendicular to the microprobe (see Fig. 1). A force-calibrated microprobe was positioned so as to impinge on the flagellum, making contact generally at a point distal to the curved midpiece. The force exerted against the calibrated microprobe was determined by measuring the lateral displacement of the probe as the sperm was moved to unbend the calcium-induced hook. To determine the probe displacement, the probe was always separated from the sperm by the lateral movement of the microscope slide. The pre-release displacement of the probe was determined relative to the post-release equilibrium position. All trials where repositioning of the probe may have occurred during or after displacement measurement (based on review of the videotape) were not used in the final data pool.

In our first set of experiments, the calibrated microprobe was used to manipulate the hook into a nearly straight position, and force was measured by the lateral displacement of the probe from its equilibrium position after release from the sperm. For the data presented here, only measurements from cells where the final curvature of the hook region was reduced to less than  $\pm 100$  radians/cm were used. The torque needed to open up the hook to a nearly straight configuration was found from this group by multiplying the measured force by the length of the lever arm to the midpoint of curvature measurement on the flagellum. The torque needed to open the calcium hooks to a straight configuration averaged  $2.6 (\pm 1.4) \times 10^{-7}$  dyne  $\times$  cm ( $n = 13$ ).

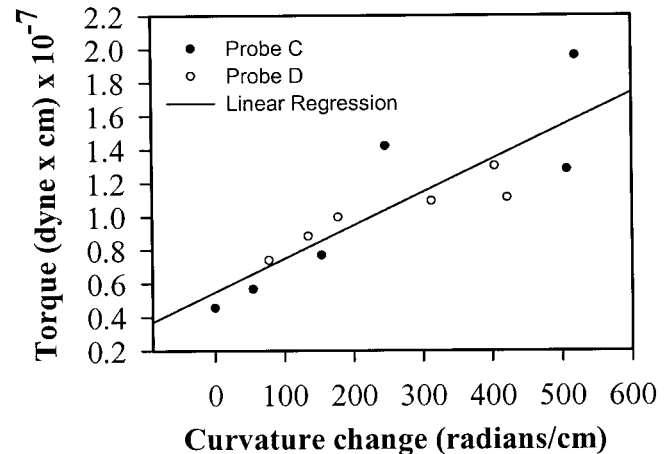


Fig. 4. The relationship of applied torque to the change in curvature measured on a single cell. The sperm was straightened out of a calcium hook in a continuous experimental operation as described in the text. The torque applied to the cell with the measurement probe is plotted as a function of the resulting decrease in the curvature of the calcium-hook. *Open circles* and *filled circles* are data obtained with two separate calibrated glass probes with very different stiffnesses (*closed circles*,  $8.76 \times 10^{-6}$  dyne/ $\mu\text{m}$ ; *open circles*,  $2.94 \times 10^{-6}$  dyne/ $\mu\text{m}$ ).

The initial curvature of the hooks varied from one sperm to another (270–1,100 radians/cm,  $n = 54$ ). Similarly, we found that there was considerable variation in the estimates of torque required to unbend the hooks, which in our sample ranged from  $8.2 \times 10^{-8}$  dyne  $\times$  cm to  $5.4 \times 10^{-7}$  dyne  $\times$  cm. There was a correlation between the initial curvature of the hook and the torque required to straighten the hook, as seen in Figure 3. Therefore, some, but not all, of the variability of the data can be attributed the tightness of the individual hooks.

A second set of experiments looked at the relationship of torque to curvature change in individual cells. Torques were found for an individual hook as it was progressively opened up by laterally moving the cell against a stationary probe. This procedure was successfully repeated on five cells, in each case yielding a linear relationship between torque and change in curvature. We saw nothing to suggest that either the force or torque reached a plateau as the degree of unbending increased.

Figure 4 shows the regression analysis obtained from a single cell measured with two different calibrated probes and demonstrates that the result is relatively independent of the specific microprobe. One of the probes used for this measurement (Fig. 4, open circles) had the best calibration statistics of all the probes used in the course of the study, with a scatter of the individual bead calibration points of  $\pm 8\%$  (mean value of  $2.94 (0.24 \pm 10^{-6})$  dynes/ $\mu\text{m}$ ,  $n = 8$ ). This best estimate yielded a torque of  $1.8 \times 10^{-7}$  dyne  $\times$  cm ( $1.8 \times 10^{-14}$  N  $\times$  m) to

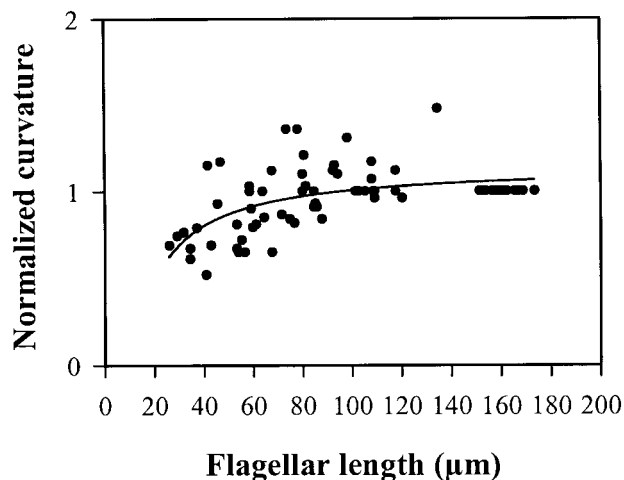


Fig. 5. A plot of normalized curvature as a function of flagellar length. The curvature at shortened lengths divided by the initial curvature of the same cell before shortening (full length) is displayed as a function of shortened length. Normalized curvature (radians/cm) decreases with decreasing flagellar length, when the flagellar length is reduced below 60–80  $\mu\text{m}$ .

open the hook, as taken from the pooled regression line. The linear relationship of torque vs. change in curvature seen in Figure 4 suggests an elastic-like behavior of the hook. These best case results are generally compatible with the torque value obtained from the larger sample ( $2.6 \times 10^{-7}$  dyne  $\times$  cm) of thirteen individual torque measurements. An estimated flagellar stiffness of  $2.9 \times 10^{-10}$  dyne  $\times$  cm<sup>2</sup> ( $2.9 \times 10^{-19}$  N  $\times$  m<sup>2</sup>) was obtained by using the regression analysis obtained from Figure 4.

To obtain a crude estimate of the portion of the flagellum that contributes the force for maintenance of the hook, sperm flagella were shortened and the pre- and post-cutting curvature of the hook was plotted as a ratio (Fig. 5). There is an obvious reduction in the post-dissection curvature of the hooks when the flagella are shortened to less than 50  $\mu\text{m}$ . The data points between 50 and 60  $\mu\text{m}$  ( $n = 9$ ) also showed a statistically significant reduction in curvature as compared to the longer segments ( $P < 0.001$ ). These results suggest that the hook is produced by force generated in the basal part of the flagellum. The data also establishes that the contributing region must be fairly long ( $>50 \mu\text{m}$ ).

The curvature of the hooked flagellum before mechanical unbending was compared to the curvature after unbending to detect any reduction in curvature as a result of unbending. The results are shown in Figure 6. It appears that there is little or no effect of mechanically unbending the hook on the subsequent curvature as the slope of the plot is 0.97. This supports the view that the hooks are highly resilient and show little plasticity.

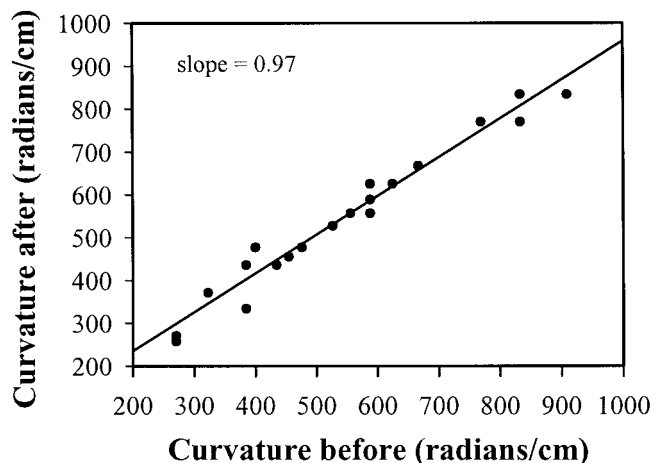


Fig. 6. Curvature (radians/cm) measurements before and after unbending calcium induced hooks of rat sperm cells. The slope of the regression line is 0.97. This indicates that the straightening of the calcium-induced hook in a rat sperm flagellum returns to its original curvature relatively consistently.

In order to obtain a benchmark, to which we may compare our data on the calcium hooks, we also measured the stiffness of the rat sperm in rigor. This was accomplished by bending the flagellum of Triton X-100 extracted rat sperm in the absence of ATP. Sperm cells do not form a calcium hook without ATP [Lindemann and Goltz, 1988]. A calibrated probe was used to bend the same region of the flagellum where the hook curvature measurements were taken. The estimated stiffness of the rigor flagellum in this region averaged  $1.8 (\pm 0.6) \times 10^{-9}$  dyne  $\times$  cm<sup>2</sup> ( $1.8 \times 10^{-18}$  N  $\times$  m<sup>2</sup>) from eight measurements. This stiffness is approximately four times greater than the apparent stiffness of the calcium hooks.

## DISCUSSION

The fishhook shape that is exhibited by rat sperm in the presence of  $1.7 \times 10^{-4}$  M free  $\text{Ca}^{+2}$  is a fairly stable conformation of the sperm flagellum. The hook holds its shape after repeated unbending with a glass microprobe and seems to be produced largely by forces developed in the basal 40 to 50  $\mu\text{m}$  of the flagellum. The torque necessary to straighten a hook is quite substantial, averaging  $2.6 \times 10^{-7}$  dyne  $\times$  cm.

This magnitude of force suggests that dynein, the primary motor protein, is likely to be involved in order to produce forces as large as those we measured. If active dynein arms were responsible for the torque development, we would expect to see a plateau of torque when the force applied by the probe exceeded the stall force of the dynein arms. Instead, our data seems to suggest a linear relationship of torque with a change in curvature.

This is a behavior exhibited by elastic structures when they are deformed. This pseudo-elastic behavior yields an estimate of the stiffness of the hooked flagellum on the order of  $4.0 \times 10^{-10}$  dyne  $\times$  cm<sup>2</sup>. This apparent Young's modulus is very high when compared to the stiffness of other cilia and flagella. It is 2,000 times the estimated passive stiffness of a simple cilium [Rikmenspoel and Rudd, 1973], and 100 times the estimated passive stiffness of a bull sperm flagellum [Lindemann et al., 1973]. However, rat sperm flagella are one of the largest of all flagella and their outer dense fibers and fibrous sheath must add substantially to the passive elastic modulus. Our measurement of the rigor stiffness confirms that the stiffness of the hook is less than can be generated by the rigor attachment of the dynein arms. Therefore, it is possible that the dynein motor proteins produce the force that forms the hook. This could be mediated by a special subset of dyneins in the proximal portion of the flagellum. This interpretation is also supported by the previous observation that high levels of vanadate will release the hooks [Lindemann et al., 1990].

If we presume that dynein is the source of the motive force in a hook, then two possible explanations could account for the elastic-like behavior of the hook. The first possibility is that in the presence of Ca<sup>+2</sup>, a subset of the dyneins could be locked in a rigor-like state that is not easily triggered to release while Ca<sup>+2</sup> is bound. Alternately, the dyneins on one side of the axoneme may be selectively induced to undergo active sliding in the presence of Ca<sup>+2</sup>. This would produce an active bending torque by interdoublesliding sufficient to bend the flagellum to the point where an equal and opposite passive elastic torque results. In this scenario, the hook is the balance position between active sliding and elastic resistance. Both possibilities are consistent with a dynein-based mechanism.

Rat sperm have a unique geometry that has allowed us to identify with certainty which set of dyneins would normally produce the force needed to bend the flagellum into a calcium-hook. The dyneins located on doublets 1,2,3, and 4, in the usual numbering convention of the axoneme, are the dyneins of the correct polarity to produce the hook force [Lindemann et al., 1990]. The elastic resistance provided by dyneins on just these doublets would be expected to be less than the elastic resistance provided by the full complement of dyneins in the rigor state.

## ACKNOWLEDGMENTS

We thank Robin M. Autore and Danial Oberski for assistance with the experiments and manuscript preparation and Steve Sapilewski, Instructional Technology Center, Oakland University for assistance with Figure 1.

This work was partly supported by a Howard Hughes Medical Institute student fellowship for M.J.M. in the Biological Communications Program at Oakland University.

## REFERENCES

- Brokaw CJ. 1979. Calcium-induced asymmetrical beating of Triton-demembrated sea urchin sperm flagella. *J Cell Biol* 82:401–411.7
- Brokaw CJ. 1987. Regulation of sperm flagellar motility by calcium and cAMP-dependent phosphorylation. *J Cell Biochem* 35:175–184.
- Brokaw CJ, Goldstein SF. 1979. Asymmetrical oscillation of sea urchin sperm flagella induced by calcium. In: Fawcett DW, Bedford JM, editors. *The spermatozoon*. Munich: Urban & Schwarzenberg, p 153–156.
- Brokaw CJ, Josslin R, Bobrow L. 1974. Calcium ion regulation of flagellar beat symmetry in reactivated sea urchin spermatozoa. *Biochem Biophys Res Commun* 58:795–800.
- Fraser L.R. 1987. Minimum and maximum extracellular Ca<sup>2+</sup> requirements during mouse sperm capacitation and fertilization in vitro. *J Reprod Fert* 81:77–89.
- Gibbons BH. 1980. Intermittent swimming in live sea urchin sperm. *J Cell Biol* 84:1–12.
- Gibbons BH, Gibbons IR. 1980. Calcium-induced quiescence in reactivated sea urchin sperm. *J Cell Biol* 84:13–27.
- Hegemann P, Bruck B. 1989. Light-induced stop response in *Chlamydomonas reinhardtii*: occurrence and adaptation phenomena. *Cell Motil Cytoskeleton* 14:501–515.
- Holcomb-Wygle DL, Schmitz KA, Lindemann CB. 1999. Flagellar arrest behavior predicted by the Geometric Clutch hypothesis is confirmed experimentally by micromanipulation experiments on reactivated bull sperm. *Cell Motil Cytoskeleton* 44:177–189.
- Lindemann CB, Goltz JS. 1988. Calcium regulation of flagellar curvature and swimming pattern in Triton X-100-extracted rat sperm. *Cell Motil Cytoskeleton* 10:420–431.
- Lindemann CB, Rudd WG, Rikmenspoel R. 1973. The stiffness of the flagella of impaled bull sperm. *Biophys J* 3:437–448.
- Lindemann CB, Goltz JS, Kanous KS. 1987. Regulation of activation state and flagellar wave form in epididymal rat sperm: Evidence for the involvement of both Ca<sup>2+</sup> and cAMP. *Cell Motil Cytoskeleton* 8:324–332.
- Lindemann CB, Goltz JS, Kanous KS, Gardner TK, Olds-Clarke P. 1990. Evidence for an increased sensitivity to Ca<sup>2+</sup> in the flagella of sperm from *t<sup>w32</sup>/+* mice. *Mol Reprod Devel* 26:69–77.
- Miller RL, Brokaw CJ. 1970. Chemotactic turning behaviour of *Tubularia* spermatozoa. *J Exp Biol* 52:699–706.
- Naitoh Y. 1968. Ionic control of the reversal response of cilia in *Paramecium caudatum*. A calcium hypothesis. *J Gen Physiol* 51:85–103.
- Naitoh Y. 1969. Control of the orientation of cilia by adenosinetriphosphate, calcium and zinc in glycerol-extracted *Paramecium caudatum*. *J Gen Physiol* 53:517–529.
- Naitoh Y, Kaneko H. 1972. Reactivated Triton-extracted models of *Paramecium*: Modification of ciliary movement by calcium ions. *Science* 176:523–524.
- Rikmenspoel R, Rudd WG. 1973. The contractile mechanism in cilia. *Biophys J* 13:955–993.

- Satir P. 1975. Ionophore-mediated calcium entry induces mussel gill ciliary arrest. *Science* 190:586–588.
- Schmidt JA, Eckert R. 1976. Calcium couples flagellar reversal to photostimulation in *Chlamydomonas reinhardtii*. *Nature* 262: 713–715.
- Schmitz KS, Holcomb-Wygle DL, Oberski DJ, Lindemann CB. 2000. Measurement of the force produced by an intact bull sperm flagellum in isometric arrest and estimation of the dynein stall force. *Biophys J* 79:468–478.
- Suarez SS, Varosi SM, Dai X. 1993. Intracellular calcium increases with hyperactivation in intact, moving hamster sperm and oscillates with the flagellar beat cycle. *Proc Natl Acad Sci USA* 90:4660–4664.
- Tsuchiya T. 1976. Ca-induced arrest response in Triton-extracted lateral cilia of *Mytilus* gill. *Experientia* 32:1439–1440.
- Tsuchiya T. 1977. Effects of calcium ions on Triton-extracted lamel-libranch gill cilia: Ciliary arrest response in a model system. *Comp Biochem Physiol* 56A:353–361.
- Van Buren P, Work SS, Warshaw DM. 1994. Enhanced force generation by smooth muscle myosin in vitro. *Proc Natl Acad Sci USA* 91:202–205.
- Wais-Steider J, Satir P. 1979. Effect of vanadate on gill cilia: Switching mechanism in ciliary beat. *J Supramol Struct* 1:339–347.
- Walter MF, Satir P. 1978. Calcium control of ciliary arrest in mussel gill cells. *J Cell Biol* 79:110–120.